

Supporting Information

Iriarte et al. 10.1073/pnas.1201461109

SI Materials and Methods.

Pollen. Pollen preparations followed standard chemical digestion procedures (1, 2), including hot treatments in 40% (wt/wt) HF and 10% (wt/vol) NaOH, and were mounted in silicone oil for analysis. Thirty horizons were analyzed separately for cultigen pollen types. To maximize the likelihood of recovering large, cultigen pollen, chemically digested sediments were passed through a 53- μm brass sieve and residues were retained for analysis. Exotic *Lycopodium* markers were added to the residues before mounting in silicone oil. Pollen slides were scanned at 100 \times magnification, and approximately the same volume of residue was scanned for cultigen pollen types at each horizon, as determined using the exotic *Lycopodium* markers. Maize (*Zea mays*) pollen was identified based on its size ($> 70 \mu\text{m}$) and the absence of wild *Zea* in the region. Phase-contrast microscopy was used to examine the exine details of large ($> 70 \mu\text{m}$) Poaceae grains to discount *Tripsacum*, a genus of wild Poaceae that produces pollen comparable in size to that of *Z. mays* (3). Pollen of *Ipomoea batatas* type and *Manihot* is indistinguishable between that of cultigens (sweet potato and manioc, respectively) and wild relatives, but we are confident that the grains we report come from cultigens for the following reasons. Only one wild *Manihot* species occurs in some coastal savannas, but has never been seen near our study site. Wild *Ipomoea* was absent from a detailed phytosociological study of Kourou savannas in the region (4). The co-occurrence of *Manihot* and *Ipomoea* pollen, as well as their close association with independent evidence of colonial land use in the study area (abundant charcoal, agricultural raised beds in forested contexts), and their absence at the site before the first signs of human land use (pre-Columbian raised-field cultivation), is most parsimoniously interpreted as evidence for sweet potato and manioc cultivation. Stratigraphic plots were created using Golden software: Grapher

(5). The terrestrial pollen sum includes Cyperaceae, as it is a dominant component of the seasonally-flooded savanna in the study area.

Phytoliths. Phytolith extractions from the K-VIII core sediment samples followed standard procedures (6). Samples were deflocculated in a shaker with Calgon for 24 h. Clays were washed by gravitational sedimentation, carbonates were removed using hydrochloric acid, and organic matter was removed with nitric acid and potassium chlorate when necessary. Samples were floated in a zinc bromide solution at a specific density of 2.3 g/mL⁻¹, dried in acetone, and mounted in Permout. To maximize the recovery of important phytoliths of different size classes, such as those that derive from the rinds of *Cucurbita* fruits and from leaves and cobs of maize (*Z. mays* L.), archaeological sediments were separated by wet-sieving into fine silt (fraction A, 2–25 μm), coarse silt (fraction B, 25–50 μm), and sand (fraction C, 50–2,000 μm) fractions. The entire extract recovered from the sand fraction was scanned to search for *Cucurbita* phytoliths and other large phytoliths of arboreal and economically important plant forms.

Charcoal. Samples for charcoal analyses were taken from contiguous 1-cm intervals over 31 cm of core. Samples were disaggregated in a hot-water bath of 5% (wt/vol) KOH for 10–20 min and washed through a 125- μm mesh screen (7). Macroscopic charcoal particles $> 125 \mu\text{m}$ were identified and tallied at 36 \times under a stereomicroscope. A total of 31 charcoal samples, averaging 28 y per sample for the last 500 y, and 77 y per sample over the 2,150-y-long record, were tallied. Raw charcoal counts were first converted to concentration (particles cm⁻³), and then to charcoal accumulation rate (particles cm⁻²y⁻¹).

1. Faegri K, Iversen J (1989) *Textbook of Pollen Analysis* (Wiley, Chichester, UK).
2. Bennett K, Willis K (2001) Pollen. Tracking environmental change using lake sediments. *Tracking Environmental Change using Lake Sediments III. Terrestrial, Algal, and Siliceous Indicators*, eds Smol JP, Birks HJ, Last WM, Bradley RS, Alverson K (Springer, New York), pp 5–32.
3. Holst I, Moreno JE, Piperno DR (2007) Identification of teosinte, maize, and *Tripsacum* in Mesoamerica by using pollen, starch grains, and phytoliths. *Proc Natl Acad Sci USA* 104:17608–17613.
4. Hoock J (1971) *The Guianan Savannas: Kourou* (Mémoires ORSTOM, Paris). French.
5. Golden Software Inc. (2011) Grapher—v. 8.8.957 Graphing System. Available at <http://www.goldensoftware.com>.
6. Piperno DR (2006) *Phytoliths: A Comprehensive Guide for Archaeologists and Paleoecologists* (AltaMira Press, San Diego).
7. Whitlock C, Larsen C (2002) Charcoal as a Fire Proxy. *Tracking Environmental Change Using Lake Sediments III. Terrestrial, Algal, and Siliceous Indicators*, eds Smol JP, Birks HJB, Last WM, Bradley RS, Alverson K (Springer, New York), pp 75–97.

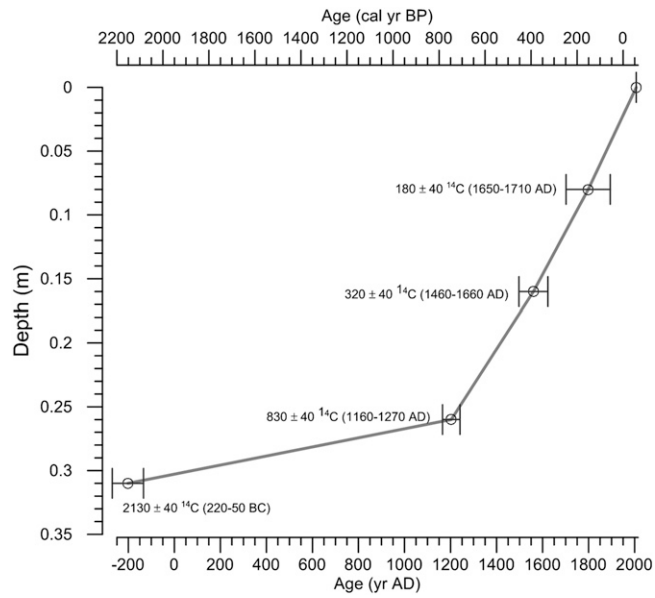


Fig. S1. Age-depth model for the K-VIII core, based on linear interpolation between four calibrated (CALIB 5.0.1) (1) radiocarbon dates (Table S1) and a top-core date of A.D. 2007, the year of core collection.

1. Stuiver M, Reimer PJ, Reimer R (1993) Calib radiocarbon calibration program. *Radiocarbon* 35:215–230.

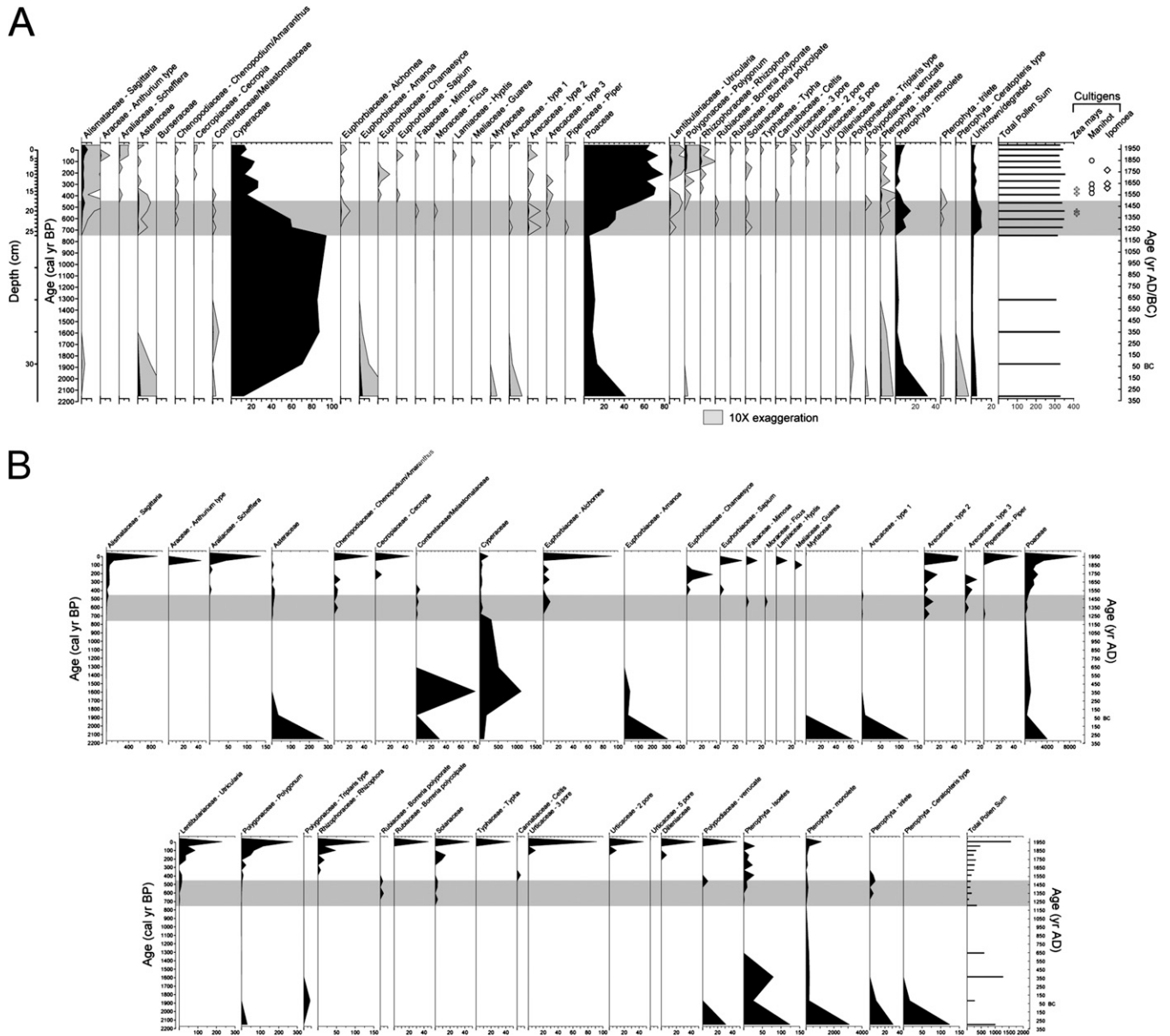


Fig. S2. Summary diagrams of pollen percentages and pollen accumulation rates. (A) Pollen percentages of selected pollen taxa from K-VIII calculated by summing all terrestrial and aquatic taxa and excluding spores of Pterophyta-types. Cultigen pollen types, not included in percentage calculations, are indicated by symbols at far right where *Ipomoea batatas* type. Gray curves to the right of solid black curves represent 10× exaggerations. (B) Pollen accumulation rates ($\text{grains cm}^{-2}\text{yr}^{-1}$) from K-VIII were calculated by using *Lycopodium* tracers in each sample to estimate changes in pollen influx per taxon independent of the percentage calculation. Gray horizontal bar represents the period of raised-field farming, A.D. 1200–1500. Pollen diagrams were created using TILIA software (1).

1. Grimm EC (1987) CONISS: A FORTRAN 77 program for stratigraphically constrained cluster analysis by the method of incremental sum of squares. *Comput Geosci* 13:13–35.

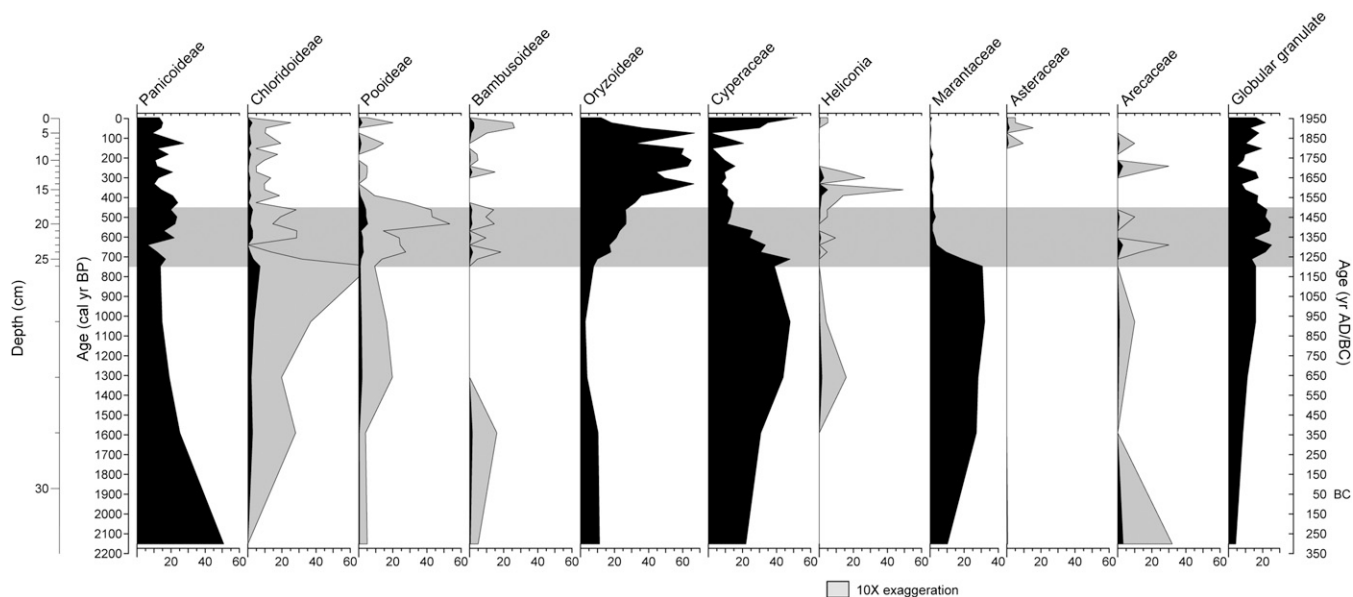


Fig. S3. Percentage phytolith diagram. Percentage of small phytoliths (Fractions A + B < 50 μm : all Poaceae, Cyperaceae, *Heliconia*, globular granulate and Arecaceae) was calculated as the percentage of the Fraction A+B sum (minimum 200 grains). Percentage of large phytoliths (Fraction C, > 50 μm : Asteraceae and Marantaceae) was calculated as the percentage of the sum of Fraction A+B plus Fraction C. Gray curves to the right of solid black curves represent 10 \times exaggerations and gray horizontal bar represents the period of raised-field farming, A.D. 1200–1500. The phytolith diagram was created using TILIA software (1).

1. Grimm EC (1987) CONISS: A FORTRAN 77 program for stratigraphically constrained cluster analysis by the method of incremental sum of squares. *Comput Geosci* 13:13–35.

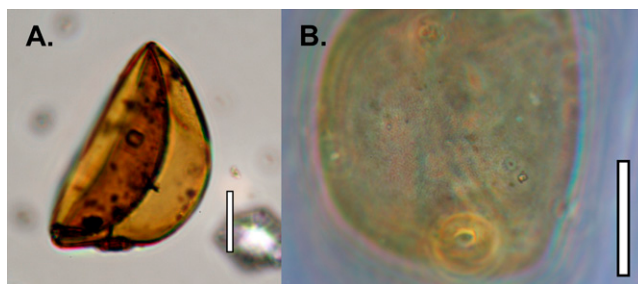


Fig. S4. *Z. mays* pollen from K-VIII 16–16.5 cm. (A) Photograph taken at 400 \times magnification under normal light microscopy; (B) the same specimen photographed under phase contrast (1,000 \times magnification) showing evenly distributed intertextile columellae, unlike large Poaceae grains of the genus *Tripsacum*, which show a clumped distribution (3). (Scale bars, 20 μm .)

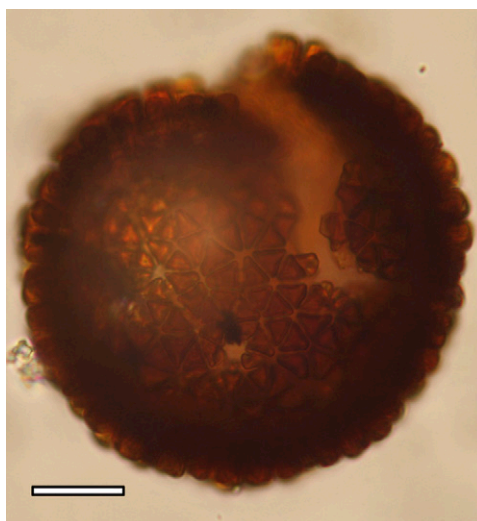


Fig. S5. *Manihot* pollen from K-VIII 14.5–15 cm. The image was created using a composite of four separate photographs (400× magnification) taken at different focal planes, and assembled using the “photo-stacking” application in Photoshop CS5. (Scale bar, 20 μm.)

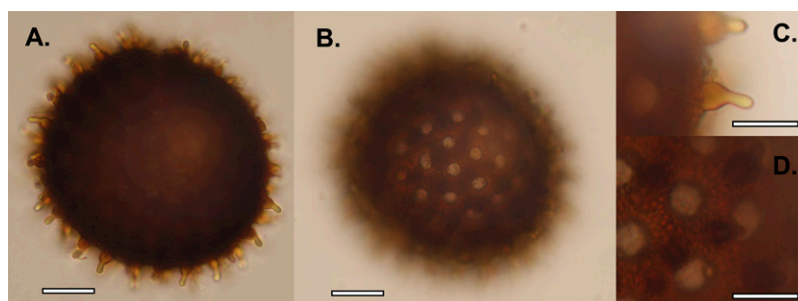


Fig. S6. *Ipomoea batatas*-type pollen from K-VIII 12–12.5 cm. Photographs taken at 400× magnification demonstrate (A) arrangement of large echinae and (B) pore size, shape, and arrangement. (Scale bars, 20 μm.) Photographs taken at 1,000× magnification show (C) detail of the bottle-shaped echinae (Scale bar, 10 μm); and (D) arrangement of large echinae around each pore, typically numbering three to five (Scale bar, 10 μm).

Table S1. Accelerator mass spectrometry radiocarbon dates from the K-VIII core

Depth (cm)	¹⁴ C age B.P.	δ ¹³ C [‰]	2 σ Calibrated A.D.	Material dated*	Lab. no.
8	180 ± 40	−26.5	Cal A.D. 1650–1710, 1710–1880, 1910–1950	Peat	Beta-282831
16	320 ± 40	−27.1	Cal A.D. 1460–1660	Peat	Beta-282832
26	830 ± 40	−26.8	Cal A.D. 1160–1270	Peat	Beta-282833
31.5	2130 ± 40	−28.7	Cal B.C.350–290, 220–50	Peat	Beta-254056

*No fine roots were encountered during the pollen preparation procedure, which incorporated a 53-μm sieving stage, so we are confident that potential contamination from modern-root carbon in the bulk peat samples can be discounted.